IN-VENTO 2026
International Conference of the Italian Association for Wind Engineering
Bari, September 13th – 16th, 2026

BARI

Investigating vertical wind angle effects using synchronous pressure and velocity data for varying roof slopes

Jihan S. Pacer[1], Gregory A. Kopp [2]

[1]University of Western Ontario, London, ON, Canada, jpacer@uwo.ca
[2]Canadian Severe Storms Laboratory, London, ON, Canda, gakopp@uwo.ca

ABSTRACT
The effects of the vertical wind angle on building surface pressures is investigated in this study. Specifically, the behaviour of the linear correction term, B(θ), which accounts for the vertical wind angle effects following the Wu & Kopp (2016) QS model was studied using the synchronous pressure and velocity data from the experiments conducted by Acosta (2024). Four different roof slopes (0°, 14°, 27° and 45°) were considered in the analysis. The term, B(θ), was determined by plotting the change in the conditionally averaged pressure coefficients with respect to the variation in the vertical wind angle. The linear plot of B(θ) showed similarity for flows governed by strong flow separation and decreases in slope as the effects of flow separation are reduced, becoming negligible for flow cases where there is no flow separation such as the windward panel for 45° roof slope with wind direction perpendicular to the ridge. It was also found that changes in pressure are more sensitive to upward wind cases as compared to downward acting winds that can be attributed to the enhanced flow separation associated with upward winds.

Keywords: Vertical Angle Effects, Quasi-steady Theory, Low-Rise Buildings, Building Aerodynamics

1. INTRODUCTION

To improve the accuracy of quasi-steady (QS) model in predicting surface pressures, past studies investigated the effects of vertical wind angle by tilting the building model in the vertical plane and subjecting it to straight-line winds. Typically, the changes in the mean pressure coefficients as function of the vertical wind angle are measured and incorporated in QS models (Richards & Hoxey, 2004, Sharma & Richards, 1999, and Letchford & Marwood, 1997). Vickery (2024) also adopted the method of tilting the building model to observe elevation angle effects and develop a factor that accounts for the effects of high vertical winds present near the tornado core when estimating tornadic wind loads using pressure coefficients obtained from straight line winds, as prescribed in the ASCE 7-22 design code. However, they extended the tilt angle up to 20° which can affect vortex structures around the building and fundamentally change the flow above the roof.

Another method of analyzing vertical wind angle effects is by conducting synchronous pressure and velocity measurements (Wu & Kopp, 2016, Guo & Kopp, 2025). This enables the evaluation of the sensitivity of pressure coefficients to changes in the vertical wind angles including steep vertical wind angles without significant disturbance to the flow around the building. Using this method, a cobra probe is placed at a point with vertical distance equal to twice the mean roof height, 2H, above the ground. This point was determined to be a location where velocity measurements are well correlated with building surface pressures while distortion of flow due to the presence of building is minimized. The cobra probe then measures the instantaneous velocity vector from which the instantaneous horizontal and vertical wind angles, θ and β, can be derived and incorporated in the QS model.

To observe how vertical wind angles affect roof pressures, this study investigates the behaviour of the change in conditionally averaged pressure coefficients, obtained from synchronous pressure and velocity data, with changes in the vertical wind angle for various roof slopes. This is done considering area-averaged roof panels with the future objective of developing a QS model that will serve as a basis for main-wind force resisting system (MWFRS) roof loads incorporating vertical wind angle effects.

2. METHODS

To understand vertical wind angle effects, this study will look into the behavior of the correction term, which was found to be linear (Wu & Kopp, 2016, Richards & Hoxey, 2004, Sharma & Richards, 1999, and Letchford & Marwood, 1997), associated with vertical wind angle, $B(\theta)$, shown in Equation 1 based on the QS model developed by Wu & Kopp (2016),

$$C_p(\theta,\beta) = C_p(\theta,\bar{\beta}) + B(\theta)\Delta\beta \quad (1)$$

where $C_p(\theta,\ \beta)$ is the instantaneous pressure coefficient as a function of the instantaneous horizontal and vertical wind angles, θ and β, $C_p(\theta,\bar{\beta})$ is the instantaneous pressure coefficient as a function of the instantaneous horizontal wind angle with respect to a mean vertical wind angle, $\bar{\beta}$, which is taken as equal to zero, $\bar{\beta}=0$, in the case of straight-line winds, $B(\theta)$ is a correction function used to incorporate the effects of changes in the vertical wind angle, and $\Delta\beta$ is the change in the vertical wind angle.

Four (4) different roof slopes will be considered in the analysis with synchronous pressure and velocity data obtained from Acosta (2024) experiment. The details of the experiment are tabulated in Table 1.

Table 1. Details of Acosta (2024) experiment

Model Scale Width (cm)	Model Scale Length (cm)	Model Scale Eave Height (cm)	Roof Slope (deg)	Wind Direction, θ, (deg)	Terrain
27.5	18.3	7.8	0,14,27,45	0°	Suburban with 38 cm barrier

Acosta (2024) conducted the test in the high-speed section of Boundary Layer Wind Tunnel II (BLWT II) at the University of Western Ontario (UWO). The test section has dimensions of 39 m in length, 3.34 m in width and 2.5 m in height. Measurements were conducted at mean azimuth equal to 0° which is at wind direction perpendicular to the shorter side of the building (18.3 cm). A Cobra probe (TFI Corp., Model #289) was placed 1H above the leading edge of the roof surface at the midplane of the short wall (18.3 cm) which was selected to obtain velocities representative of the flow at the building location while minimizing effects induced by the presence of the building. The model was subjected to a suburban terrain created by distributing the roughness elements on the tunnel floor between the inlet and the building location. Three 122-cm tall spires and a 38-cm tall barrier were also placed at the inlet of the tunnel.

3. RESULTS

Considering the dataset from experiments conducted by Acosta (2024), a plot of the change in the instantaneous pressure coefficient, $\Delta C_p(\theta,\beta) = C_p(\theta,\beta) - C_p(\theta,\bar{\beta})$, versus the change in the vertical wind angle, $\Delta\beta$, corresponding to windward (left) and leeward panels (right) at 0° wind direction for different slopes is shown in Figure 1. The data points represent the change in the conditionally averaged pressure coefficient, $\Delta C_p(\theta,\ \beta)$, with the pressure coefficient obtained by conditional averaging method considering bandwidths of $\pm 2.5°$ for the fluctuations in the horizontal wind angle, $\theta' = \theta - \bar{\theta}$ and $\pm 0.5°$ was used for the vertical wind angle, $\beta' = \beta - \bar{\beta}$. The data points corresponding to 0°, 14°, 27°, and 45° roof slopes are denoted by the following markers: black hollow circle, blue plus, red cross, and green hollow square. The color intensity indicates the number of data points included in the conditional averaging, which also represents the effective duration of the flow at a given vertical wind angle, ranging from 0 to more than 3 s.

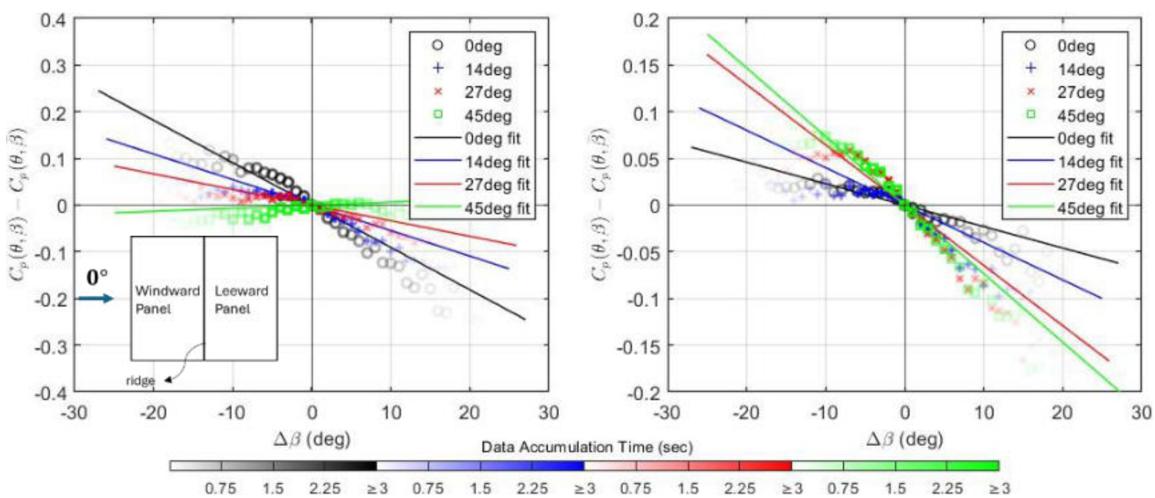

Figure 1. Plot of the changes in the conditionally averaged pressure coefficients versus the changes in the vertical wind angle, representing $B(\theta)$ for windward (left) and leeward (right) panels at 0° wind direction using Acosta (2024) data. Sketch of the wind direction, windward and leeward panels are shown in the bottom of the left panel.

From the figure, one can see that across all roof slopes, majority of the datapoints collected fall into the range of $-10° \leq \Delta\beta \leq 10°$ as can be seen in the color intensity of the markers that gradually fades for $\Delta\beta \leq -10°$ and $\Delta\beta \geq 10°$. Whereas the solid lines denote the linear fit of the data points, with the black, blue, red, and green lines corresponding to roof slopes of 0°, 14°, 27°, and 45°, respectively. These lines illustrate the $B(\theta)$ trend for each roof slope, and their slopes indicate the corresponding $B(\theta)$values.

For both the windward and leeward panels, linearity of the datapoints is observed within $0° \leq \Delta\beta \leq 10°$ except for the 45° roof slope in the windward panel. In the range of $\Delta\beta < -10°$, the datapoints for downward winds (-Δβ) tends to show constant behavior but it emerges earlier for 14° and 27° roof slopes appearing at around $\Delta\beta \approx -3°$ considering windward panel and occurring at about the same value of $\Delta\beta$ for 0° and 14° roof slopes in the case of leeward panel. For $\Delta\beta > 10°$, linearity of datapoints are observed across all roof slopes except again for the 45° roof slope in the windward panel. Though, it can be recognized that as the vertical wind angle gets higher, the datapoints become more scattered and exhibit lower color intensity, indicating less data used for conditional averaging and, consequently, increased uncertainty.

From the behaviour of the change in the conditionally averaged pressure coefficient, it can be observed that it is similar for flows associated with strong flow separation as can be seen from the $B(\theta)$ plot at the windward panel of 0° roof slope and the $B(\theta)$ plots at the leeward panel of 27° and 45° roof slopes so that $B(\theta) \approx 0.01$ for the three plots. In the case of windward panel at 0° roof slope, the flow separates due to the presence of the leading edge of the roof while in the case of leeward panel at 27° and 45° roof slopes, the flow separates due to the presence of the ridge. As the effects of flow separation is diminished, which happens at the windward panel with increasing roof slope and at the leeward panel with decreasing roof slope (thereby reducing ridge-induced effects), the variation in pressure lessens, effectively reducing the value of $B(\theta)$. Moreover, it can be noted that the changes in pressure is more affected by the changes in the upward wind as compared to downward ones as suggested by the more evident constant trend in $-\Delta\beta$ region, this suggests that upward winds promote flow separation whereas downward winds tend to stabilize the flow by reducing separation lengths to some extent (for $-3° \leq \Delta\beta \leq 0°$). As a result, suction pressures decrease and a positive change in pressure is observed. For larger $-\Delta\beta$ values, however, the minimal variation in pressure with changing vertical wind angle indicates that the associated separation lengths likely remain relatively unchanged.

4. CONCLUSION

The behaviour of the linearized correction term, $B(\theta)$, which accounts for the vertical wind angle effects following the Wu & Kopp (2016) QS model was observed for varying roof slopes. It was determined that the $B(\theta)$ associated with strong flow separation are similar to one another. As the effects of flow separation are reduced due to changes in the building geometry such as increasing roof slope in the windward panel and decreasing roof slope in the leeward panel, the $B(\theta)$ value lessens so that at the windward roof panel for 45° roof slope, it becomes negligible. It can also be noted that upward winds produce greater changes in pressure as compared to downward winds. This is because upward winds enhances flow separation causing increase in suction pressures whereas downward winds reduces separation lengths and promote flow reattachment thereby lowering suction pressures. However, it was observed that for large magnitude $-\Delta\beta$ values, there is little to no change in pressures suggesting the saturation of the reduction in separation lengths caused by downward acting winds.

ACKNOWLEDGEMENTS

This work was partially funded by the Natural Science and Engineering Research Council of Canada through the Discovery Grants program and ImpactWX through the funding to the Canadian Severe Storms Laboratory. The authors are grateful to many colleagues for helpful discussions including Dr. Jin Wang, Dr. Yitian Guo, Dr. Stefano Brusco, and Mr. Tim Acosta.

REFERENCES

Acosta, T. (2024). Effects of geometry and turbulence on the horseshoe vortex and windward loads of low-rise buildings [Manuscript in preparation]. Department of Civil and Environmental Engineering. University of Western-Ontario.

Guo, Y. and Kopp, G. A. (2025). The application of the quasi-steady vector model to low-rise buildings with sloped roofs. Journal of Wind Engineering and Industrial Aerodynamics, 259, 106056.

Letchford, C.W. and Marwood, R. (1997). On the influence of v and w component turbulence on roof pressures beneath conical vortices. Journal of Wind Engineering and Industrial Aerodynamics, 69-71: 567-577.

Richards, P.J. and Hoxey, R.P. (2004). Quasi-steady theory and point pressures on a cubic building. Journal of Wind Engineering and Industrial Aerodynamics, 92(14-15): 1173-1190.

Sharma, R.N. and Richards, P.J. (1999). The influence of Reynolds stresses roof pressure fluctuations. Journal of Wind Engineering and Industrial Aerodynamics, 83: 147-157

Wu, C.-H.and Kopp, G.A. (2016). Estimation of Wind-Induced Pressures on a Low-Rise Building using Quasi-Steady Theory. Frontiers in Built Environment, 2:5.

Vickery, P.J. (2024). Personal Communication.